ORIGINAL RESEARCH PAPER
Volume - 14 | Issue - 07 | July - 2025 | PRINT ISSN No. 2277 - 8179 | DOI : 10.36106/ijsr
INTERNATIONAL JOURNAL OF SCIENTIFIC RESEARCH

BIOCOMPATIBLE GSH-COATED CDS/ZNS QUANTUM DOTS FOR FLUORESCENT IMAGING OF CANCER AND EPITHELIAL CELL LINES

Biotechnology

Rama Siripelly Research Scholar, Department of Biotechnology, OU.

P. Pushpalatha Assistant Professor of Biotechnology, 2Government Degree College for Women (A), Nalgonda, India.

Anupalli Roja Rani* Professor in Genetics & Biotechnology. *Corresponding Author

ABSTRACT

The present paper presents the development and characterization of glutathione-coated CdS/ZnS core-shell quantum dots (QDs) for biocompatible cellular imaging and targeting. CdS/ZnS quantum dots were produced using a one-pot high-temperature technique and made water-soluble through ligand exchange with DL-cysteine. Glutathione (GSH) was coupled by EDC/NHS chemistry to enhance stability and biocompatibility, resulting in quantum dots (QDs) with a hydrodynamic diameter of approximately 20 nm, robust blue fluorescence emission at 455 nm, and a quantum yield of 39%. FTIR validated the effective alteration of the GSH surface. MTT studies on MCF-7 and HeLa cells revealed robust cell viability (>90%) at doses up to 10 µg/mL, signifying little cytotoxicity. Confocal imaging demonstrated effective cellular absorption, whereas antibody (EpCAM) conjugation facilitated target labeling and flow cytometric sorting of circulating tumor cells. The GSH-coated quantum dots provide a durable, low-toxicity substitute for conventional fluorophores in cellular imaging and cancer cell identification.

KEYWORDS

CTC, Cancers, Ligand exchange, Glutathione, Metastasis, Quantum dots

INTRODUCTION

The unique size-dependent optical features of semiconductor nanocrystals also known as quantum dots (QDs) have become one of the most appealing subjects of contemporary research from past few decades (Pu et al. 2018; Zhao et al. 2018). QDs have superior optical features to typical traditional fluorophores, such as large quantum yields, broad absorption spectra, narrow and symmetric size-tunable emission, and great photobleaching resistance, making them ideal for biosensing application(Zheng et al. 2007b). The quantum confinement effect causes the size-tunable absorption and luminescence spectra of QDs(Liu et al. 2007; Matea et al. 2017).

Due to their outstanding tunable optical characteristics ofCdSe (Liu et al. 2018; VanWie et al. 2019), CdS (Jiang et al. 2007; Cui et al. 2018), CdTe(Yu et al. 2003; Zheng et al. 2007a) etc., semiconducting nanocrystals have attracted a lot of attention(Nikazar et al. 2020). The cytotoxicity of QDs is determined by various parameters, including their size, chemical composition, capping agent, and surface chemistry, as well as ambient circumstances (light, temperature, oxidative conditions)(Mirnajafizadeh et al. 2019; Shivaji et al. 2019). Multiple studies have shown that the capping ligand, and thus the surface charge, has a major impact on the cytotoxicity of QDs, with positively charged QDs being more hazardous than negatively charged QDs(Hu et al. 2019).

In other research, the role of surface chemistry and QD size in affecting QD cytotoxicity was also underlined. Cadmium species formed by surface oxidation are thought to be the cause of QDs toxicity(Deng et al. 2009). In biological applications, QDs with cadmium have a negative cytotoxicity effect, which can be minimized by surface modifications and the use of appropriate ligands(Das and Dutta 2021). The surface ligands of QDs in organic solvents make conjugations and direct cell imaging impossible. Passivation of thiolate ligands such as 3-Mercaptopropionic acid (MPA) (Sajwan et al. 2017; Hao and Liu 2019), Dihydrolipoic acid (DHA)(García-Cortés et al. 2017; Drozd et al. 2020), DL-Cysteine (CYS)(Liu et al. 2007; Li et al. 2017), Glutathione (GSH)(Aydemir et al. 2020; Tan et al. 2014; Beato-López et al. 2017), and others Polyethylene glycol (PEG) (Geng et al. 2017; Ali et al. 2019), D-Penicillin amine (DPA) (Ngamdee et al. 2017), etc., can be used to establish compatibility, according to current studies.

Glutathione (GSH) is a thiol-containing important biological oligopeptide that can be used to make functionalized QDs because it contains active carboxylic and amino groups that chelate with Cd ion with exceptional affinity, resulting in QDs that are much more biocompatible than other water soluble QDs.Other options for overcoming the compatibility concerns and making QDs available for direct cell imaging are being investigated(Milenković et al. 2021; Vaishnavi and Renganathan 2020).

In this study, we designed stable, non-toxic, and high brightness glutathione surface functionalized QDs through methods facilitated with EDC/NHS reaction, which are highly biocompatible for bioimaging and cell sorting methods.

Methodology

Chemicals And Materials

Cadmium oxide-99% (CdO), Zinc acetate-99% (Zn (Act)2), Oleic acid(OA), Sulfur powder-99% (S), DL-Cystine hydrochloride (CYS), N-hydroxy-succinimide-98% (NHS) are purchased from the Sigma-Aldrich, 1-Octadecene-90% (ODE) obtained from AcrosOrganics, Chloroform ($CHCl_3$), Acetone ($(CH_3)_2CO$), isopropanol (ISP),Methanol (CH_3OH)are purchased from J.T.Baker,1-ethyl-3-[3-dimethylaminopropyl] carbodiimide-98% (EDC) purchased from the TokyoChemical Industry Co, and Glutathione was purchased from Merck Millipore.

Synthesis of CdS/ZnS Quantum dots

For the synthesis of the of QDs we opted the previous published methodology from our lab by Vyshnava et al., 2020 (Vyshnava et al. 2020). In a typical method we prepared two reaction mixtures in threenecked flasks labelled as SOL A which with contents include 10 mM Zn (Act)2and 1 mM CdO. To consider the crystal growthfor specific emission wavelength, we used the CdO concentrations at 1.0 mM in 7 ml OA and 15 mL of 1-ODE, the reactants were allowed to stir atroom temperature for 30 min followed by gradual rise in thetemperature to 150 °C for 1 hr under nitrogenpurging. The SOL B contents 2 mM S powder was dissolved in 8 ml 1-ODE followed by heating the reactantsat 120 °C under nitrogen purging. The temperature of SOL A was set at 310 °C under nitrogen purging,and 2.0 ml of SOL B was added to SOL A with a syringe pump.The reaction was allowed for 15 min for ZnS shellsto overgrow. The reaction was carried out for 2 h, later stopped by removing the heating mantle, followed by excess ethanol addition to precipitate outthe. By using Hexane: Ethanol (1:4) the are purified to remove the excess surfactants and residual ions. Thepowder were stored at 4 °C for further usage.

Preparation Of Water-soluble Quantum Dots

with water-solubility are made possible through surface ligand exchange with DL-CYS as per availableliterature of Liu et al., 2007(Liu et al. 2007) and Milenkovic et al., 2021(Milenković et al. 2021) with few modifications in the reaction procedure.In this reaction 1mg of OA capped added to the 1 mL of $CHCl_3$, added to the 1mL of 1µg/mL DL-CYS in phosphate buffered saline (PBS) to produce ligand exchange with a biphasic phase. At room temperature, the biphasic mixture was rapidly agitated, and phase transfer of were precipitated twice with ethanol and then redispersed in PBS (pH 7.4). To this solution add 10 µL dithiothreitol (DTT), to avoid cysteine dimers production and stored in the dark at 4 °C.

Preparation of GSH coated quantum dots

To enhance the stability and the binding efficacy of the were conjugated with GSH. The protocoldeveloped by reports from literatures Park et al., 2021 (Park et al. 2021) wereused in the present study. The EDC/NHS coupling procedure was opted, where the carboxyl group of Glutathione (GSH) was conjugated onto the surface of. 1mM of GSH was combined with 5 mL of Millipore grade water (pH was adjusted to 14.7), Later 2.5 mM EDC and 5 mM NHS in MES buffer was prepared. In the dark, the mixture containing equimolar ration of EDC and NHS solution was added to the GSH solution followed by stirring for 15 minutes at room temperature. Later1 mL of solution was added and then stirred for 4 hours. The resultant solution was centrifuged for 10 minutes at maximum rpm to remove any unreactedreactants. The were kept at 4°C for future purpose.

Cell Culture And Cytotoxicity Of GSH Capped Quantum Dots

To assess the cytotoxicity of the. After overnight incubation, the supernatant was removed followed by1xPBS washing the cells. To test percentage of cell viability, the microtiter plates with cells are treated with 100µL MTT solution (0.5mg/mL in 1xPBS) and incubated at 37°C for 4 hours. Later the formazan crystals formed by individual cell lines are dissolved with 100µL dimethyl sulfoxide (DMSO), and measured the optical absorbance at 490nm ((Thermo ScientifcMultiskan Go).

Cell imaging

MCF-7, HELA and HEK-293 cell lines were grown on a six well plate with coverslips inDulbecco's Modified Eagle Medium (DMEM) (which are dissolved with 1% antibiotics penicillin/streptomycin100 U/ml and 10% fetal bovine serum), followed by incubation at 37°C in humidified 5% CO_2 The respective cell lines were treated 1µg/mL of, and allowed to incubate for 15, 30, 45 and 60 minutes of period.Later coverslips were carefully removed, and washed twice with 1xPBS, and add 1 mL of 1xPBS on the imaging screw-based chamber. Images were captured using a 405nm laser excitation source on a confocal laser scanning microscope along with (DIC) (FV1000, Olympus).

Flow cytometry

Flow cytometry sorting of the MCF-7 and THP-1 cell lines are performed usingthe two QDs with varying emission intensities, and . The method of preparation of antibodies Anti-EpCAM (Positivefor the cells with epithelial cell adhesion molecules likecirculating tumor cells eg: MCF-7 cells)and Anti-CD45 (Positive for the macrophages eg: THP-1 cells) are mentioned elsewhere in the Vyshnava et al., 2020. Individual cell lines were trypsin zed after 24 hours of growth and the free cellsare collected in the vials followed by incubation with the respective QDs. In this article we optimized two color panel analysis for sorting the cells, which excluded the dead cellsand the smaller cellular and particular debris through system-based gating. The data was acquired by passing the cellular systems with specific QDs binding on the specific lines through the flow cytometer (LSR II BD Flow analyzer),configured as per the manual provided by the instrumentmanufacturer, and the raw data were analyzed by FlowJointerface software.

RESULTS AND DISCUSSION

Figure 1(a) display the transmission electron microscopic (TEM) images of , which are merely circular in shape with well dispersed in crystalline structures with 8± 2.0nm in size. Fine atomic crystalline arrangement with 2.4Å interplanar distance was observed, the planes were identified with electron diffraction (EDS) shows (111), (220) and (311) with zinc blend structure was shown in figure 1(b), which are consistent with the previous results shown in Vyshnava et al., 2020 (Vyshnava et al. 2020), and Shivaji et al., 2019 (Shivaji et al. 2019). As with the EDS results same planes for the crystals are identified with X-ray diffraction (XRD) spectrum as referred in figure 1(c). The morphological size distribution of were studied with dynamic light scattering (DLS) shown in figure 1(d) with hydrodynamic size ranges in 8± 3.0nm, which are consistent with the TEM results.

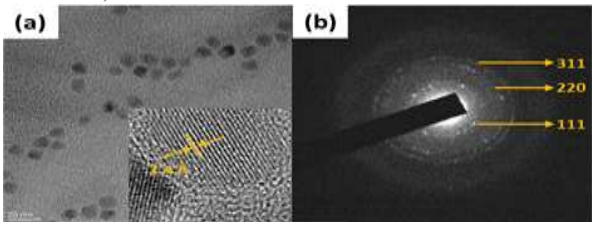

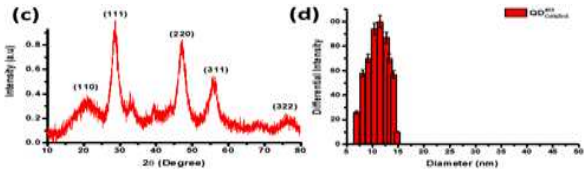

Figure 1. Morphological characterization of (a) Transmission electron microscopic images, where nanoparticle size distribution 8± 2.0nm spherical form, insight shown the crystalline positions of the atoms in nanoparticles at 5nm size (b) Electron diffraction image shown the planer positions at (111), (220), (311) were shown (c) X-Ray diffraction images shown the planer positions shown at (111), (220), (311) (d) Dynamic light scattering histogram shows the hydrodynamic size distribution of the nanoparticles at 8± 3.0nm

Figure 2 shows the absorbance and fluorescence emission spectrum of which was exited with 405 nm laser, to show maximum peak emission at 455 nm with narrow emission range for bright blue color with a quantum yield of ϕ 79% (Compared with Quinine Sulfate ϕ 96% in n-Hexanes). These shown the half life of τ15.32 ns with time resolution spectrum which is characteristic for quantum dots which are lower half life for the traditional organic dyes.

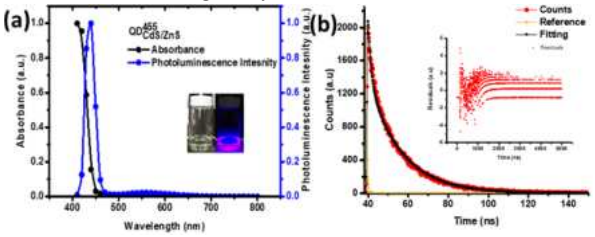

Figure 2. Ultraviolet-visible spectroscopy of (a) Absorbance and fluorescence spectrum with maximum fluorescence peak at 455nm, insight shows the blue fluorescence (b) Time resolution decay of the fluorescence halftime at 15.34 ns

As prepared were subjected to ligand exchange with DL-CYS under biphasic mixture of solvents, where the figure 3(a) shows the absorbance and fluorescence emission spectrum with peak maximum at 455 nm bright blue emission with ϕ 39% Quantum yield. This implies that the hydrophilic CYS surface ligand effectively covers the surface of the, keeping the particles stable in water and preventing aggregation in the presence of DTT. The hydrodynamic size distributions of about 15± 3.0nm shown in figure3(a) with negative charge with -19.46 mV, characteristic for presence of net negative charge on the surface of the. Later to enhance the stability and biocompatibility of the were conjugated with GSH tripeptide by using EDC/NHS coupling, the successful conjugation results were displayed in figure 3(b). The absorbance and fluorescence emission are still intact after conjugation with brighter blue emission and the hydrodynamic size ~20±4.0 nm was shown in the figure 3(b) with net negative charge -18.09 mV. The successful CYS ligand exchange and GHS conjugation were inferred by the FTIR data as shown in the figure 4 for specific wavenumber peaks for -SH, -OH, -C=O functional groups based on the available data (Liu et al. 2007; Li et al. 2017).

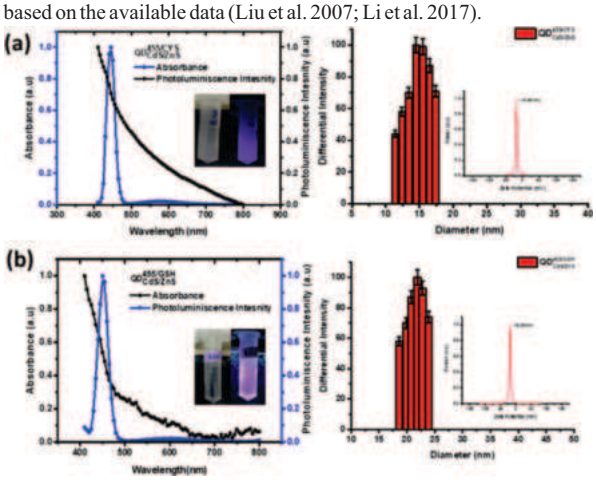

Figure 3. Surface ligand modified [QD]_(CdS/ZnS)^455 (a) Absorbance and fluorescence spectrum of QD_(CdS/ZnS)^

(455/CYS) with maximum fluorescence peak at 455nm, insight shows the blue fluorescence (b) Absorbance and fluorescence spectrum of [QD]_(CdS/ZnS)^(455/GSH) with maximum fluorescence peak at 455nm, insight shows the blue fluorescence (c) Dynamic light scattering histogram of [QD]_(CdS/ZnS)^(455/CYS) shows the hydrodynamic size distribution of the nanoparticles at 15± 3.0nm (d) Dynamic light scattering histogram of [QD]_(CdS/ZnS) ^(455/GSH)shows the hydrodynamic size distribution of the nanoparticles at 20± 4.0nm

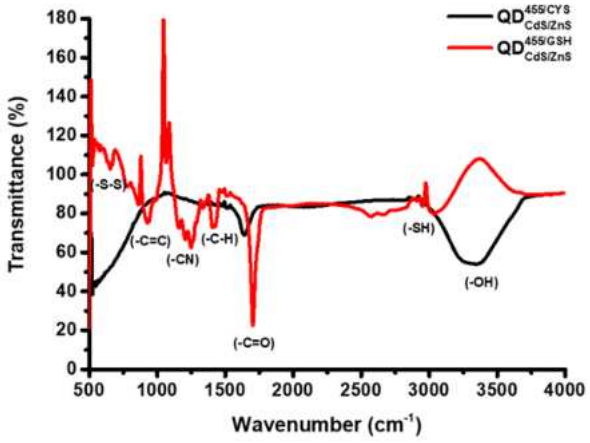

Figure 4. Fourier transform infrared spectroscopy of surface modified and

For 24 hours, HELA and MCF-7 cell lines were treated with various doses of pure and nanoparticles to investigate the effect of nanoparticle concentration. The experiment results indicated that may be less harmful than. Cell survival rates of HELA cells treated with were significantly lower than those of at all doses tested. When the concentration of was increased to 10 µg/mL, cell viability remained only 91%. In comparison, even at particle loadings of 10 µg/mL, maintained higher than 90% cell viability. After incubation with either of these QDs, no substantial cell death was seen at less than 10 µg/mL. According to these experimental findings, and appear to have a negligible harmful effect on cells and a negligible toxic effect on cells, respectively. The first reason is because, in comparison to other thiol ligands, GSH is a harmless reagent for the synthesis of aqueous QDs. Recent research indicates that the cytotoxicity of QDs may be mostly due to their surface ligands rather than the QDs themselves(Mirnajafizadeh et al. 2019; Shivaji et al. 2019). The second explanation was that the CdTe core of was sufficiently encapsulated with GSH to prevent harmful free Cd2+ emission. Finally, the significantly decreased cytotoxicity of was due to the GSH coating's efficient inhibition of QDs dissolution. Due to the short refluxing period of, their free Cd2+ content was significantly higher than that of. Additionally, were not sufficiently passivated by a GSH shell. Similar results were found in experiments with MCF-7 cell lines. Due to the fact that GSH is mostly prevalent in the cytosol and other aqueous phases of living systems, it is extremely biocompatible to use GSH stabilized QDs as biological probes(Nikazar et al. 2020; Ali et al. 2019).

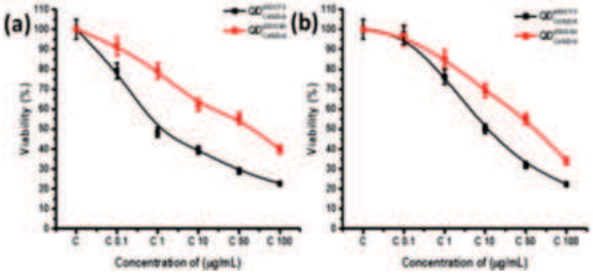

Figure 5. MTT Assay for and (a) MCF-7 cell lines (b) HELA cell lines.

The cellular imaging of the, which are incubated on theMCF-7 and HELA cell line,followed by incubation in the cells grown on the 24 mm coverslip,for 5–30 min. The morphology and distribution of the QDsuptake cell lines were observed under the confocal microscope at 40Xobjective lens equipped with 405 nmexcitation laser. Figure 6(a) and (b) display the bright blue fluorescence of the, of the HELA and MCF-7.

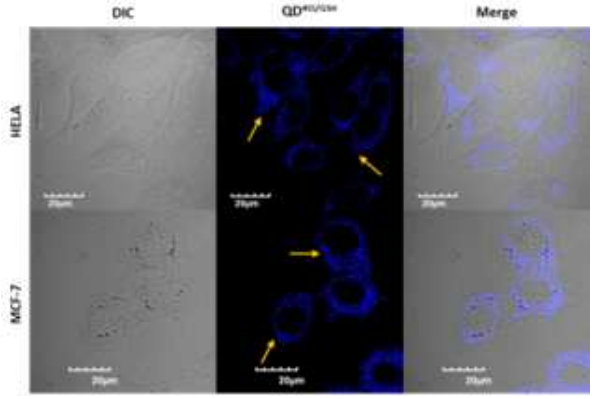

Figure 6. Confocal microscopic images of of HELA and MCF-7 cells with surface modified

Figure 7 shows the QDs are also more biocompatible than other water-soluble QDs. EpCAM was covalently coupled with biotin streptavidin paired on to the to examine the QDs' potential utility in cancer cell imaging. It is well established that the EpCAM receptor is overexpressed in a range of neoplastic tissues, including ovarian, breast, colorectal, circulating tumour, and other human cancers. It may be a target for tumor-specific diagnostic imaging. cells were incubated with MCF-7 and THP-1 under physiological circumstances, whereas cells were incubated with THP-1. MCF-7 cell lines have been shown to contain abnormally high numbers of EpCAM receptors, whereas CD45 is expressed on the surface of THP-1 cells. After various incubation times, the cells were washed three times with PBS and sorted using a flow cytometer equipped with 405nm excitation lasers. The cells were sorted according to the presence of (blue fluorescence) or (green fluorescence) on their surface. While the QDs rapidly adhere to the cell surface, considerable fluorescence can be noticed within an hour. Blue fluorescence is clearly visible on the surface of theMCF-7, whereas green fluorescence is seen on the surface of THP-1, indicating that specific binding occurs via the EpCAM and CD45 receptors.

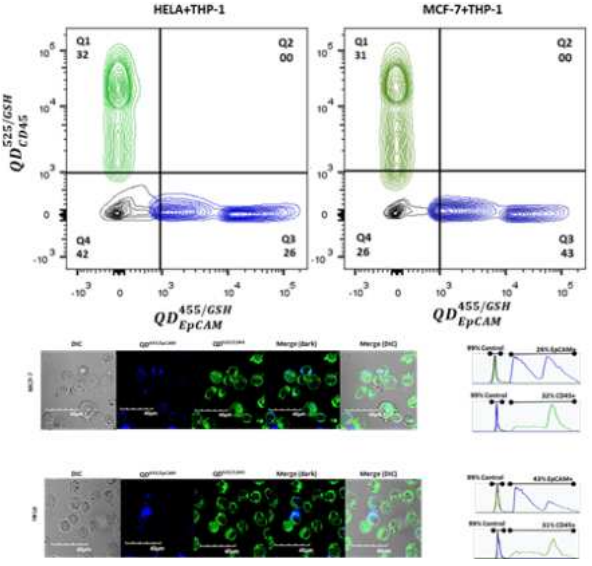

Figure 7. Flow cytometry histogram and dot plot images of HELA and THP-1 cells treated $QD_{EpCAM}^{455/GSH}$ and $QD_{CD45}^{525/GSH}$

In comparison to previous studies on CTC cell capture, our results using a standard plot for the capture of Anti-EpCAM antibody positive MCF-7 cells with conjugate are encouraging for further developing the isolation of rare cancer cell populations such as CTC and other antibody specific cancer cells that extend in the spectral space for imaging and multiplex sorting of the cells.

CONCLUSION

In this study, we effectively synthesized stable blue with narrow emission intensity at 450 nm wavelength. The CYS surface ligand

exchange makes it possible for these QDs to be stable in aquatic environments. Furthermore, the GSH coating improved the stability. Confocal imaging was used to illustrate the ability of cellular uptake in MCF-7 and HELA cell lines with the highest contrast and visibility in the cells. Additionally, sorting of EpCAM positive cell lines was accomplished by, for MCF-7. We proved the accessibility of a new stable quantum dot with brighter emission intensities based on the findings, which has significant implications for cellular imaging, targeting, and sorting research with low cytotoxicity.

Acknowledgements

The authors gratefully acknowledge the Department of Biotechnology, Faculty of Science, Osmania University, Hyderabad, for their continuous moral support and encouragement throughout the research. We also extend our sincere thanks to the Central Instrumentation Facility, Osmania University, for providing the necessary instrumentation and analytical resources to carry out this study successfully.

Funding

This research received no specific grant from any funding agency in the public, commercial, or not-for-profit sectors.

Competing Interests

The authors declare that they have no known competing financial interests or personal relationships that could have appeared to influence the work reported in this manuscript.

Author Contributions

Rama Siripelly carried out experimental work and data analysis. Anupalli Roja Rani supervised the project, contributed to the conceptual design, and finalized the manuscript. All authors reviewed and approved the final version of the manuscript.

REFERENCES

1. Ali, M., Zayed, D., Ramadan, W., Kamel, O. A., Shehab, M., & Ebrahim, S. (2019). Synthesis, characterization and cytotoxicity of polyethylene glycol-encapsulated CdTe quantum dots. *International Nano Letters, 9*(1), 61–71. https://doi.org/10.1007/s40089-018-0258-6
2. Aydemir, D., Hashemkhani, M., Acar, H. Y., & Ulusu, N. N. (2020). Evaluation of the biocompatibility of the GSH-coated Ag2S quantum dots in vitro: A perfect example for the non-toxic optical probes. *Molecular Biology Reports, 47*, 4117–4129. https://doi.org/10.1007/s11033-020-05500-z
3. Beato-López, J., Espinazo, M., Fernández-Ponce, C., Blanco, E., Ramírez-del-Solar, M., Domínguez, M., García-Cózar, F., & Litrán, R. (2017). CdTe quantum dots linked to glutathione as a bridge for protein crosslinking. *Journal of Luminescence, 187*, 193–200. https://doi.org/10.1016/j.jlumin.2017.03.038
4. Cui, Y., Zhang, C., Song, L., Yang, J., Hu, Z., & Liu, X. (2018). Facile synthesis of near-infrared emissive CdS quantum dots for live cells imaging. *Journal of Nanoscience and Nanotechnology, 18*(4), 2271–2277. https://doi.org/10.1166/jnn.2018.14107
5. Das, D., & Dutta, R. K. (2021). Photoluminescence lifetime based nickel ion detection by glutathione capped CdTe/CdS core-shell quantum dots. *Journal of Photochemistry and Photobiology A: Chemistry, 416*, 113323. https://doi.org/10.1016/j.jphotochem.2021.113323
6. Deng, Z., Lie, F. L., Shen, S., Ghosh, I., Mansuripur, M., & Muscat, A. J. (2009). Water-based route to ligand-selective synthesis of ZnSe and Cd-doped ZnSe quantum dots with tunable ultraviolet A to blue photoluminescence. *Langmuir, 25*(1), 434–442. https://doi.org/10.1021/la803367f
7. Drozd, D. D., Pidenko, P. S., Presnyakov, K. Y., Strokin, P. D., & Speranskaya, E. S. (2020). Dihydrolipoic acid coated alloyed quantum dots. In *Saratov Fall Meeting 2019: Optical and Nano-Technologies for Biology and Medicine* (Vol. 11457, p. 1145714). SPIE. https://doi.org/10.1117/12.2566383
8. García-Cortés, M., Fernández-Argüelles, M. T., Costa-Fernández, J. M., & Sanz-Medel, A. (2017). Sensitive prostate specific antigen quantification using dihydrolipoic acid surface-functionalized phosphorescent quantum dots. *Analytica Chimica Acta, 987*, 118–126. https://doi.org/10.1016/j.aca.2017.07.003
9. Geng, S., Lin, S. M., Li, N. B., & Luo, H. Q. (2017). Polyethylene glycol capped ZnO quantum dots as a fluorescent probe for determining copper (II) ion. *Sensors and Actuators B: Chemical, 253*, 137–143. https://doi.org/10.1016/j.snb.2017.06.061
10. Hao, M., & Liu, R. (2019). Molecular mechanism of CAT and SOD activity change under MPA-CdTe quantum dots induced oxidative stress in the mouse primary hepatocytes. *Spectrochimica Acta Part A: Molecular and Biomolecular Spectroscopy, 220*, 117104. https://doi.org/10.1016/j.saa.2019.117104
11. Hu, L., Zhong, H., & He, Z. (2019). The cytotoxicities in prokaryote and eukaryote varied for CdSe and CdSe/ZnS quantum dots and differed from cadmium ions. *Ecotoxicology and Environmental Safety, 181*, 336–344. https://doi.org/10.1016/j.ecoenv.2019.06.039
12. Jiang, C., Xu, S., Yang, D., Zhang, F., & Wang, W. (2007). Synthesis of glutathione-capped CdS quantum dots and preliminary studies on protein detection and cell fluorescence image. *Luminescence, 22*(5), 430–437. https://doi.org/10.1002/bio.1051
13. Li, L.-L., Cui, Y.-H., Chen, J.-J., & Yu, H.-Q. (2017). Roles of glutathione and L-cysteine in the biomimetic green synthesis of CdSe quantum dots. *Frontiers of Environmental Science & Engineering, 11*(6), 1–9. https://doi.org/10.1007/s11783-017-0992-1
14. Liu, W., Choi, H. S., Zimmer, J. P., Tanaka, E., Frangioni, J. V., & Bawendi, M. (2007). Compact cysteine-coated CdSe (ZnCdS) quantum dots for in vivo applications. *Journal of the American Chemical Society, 129*(47), 14530–14531. https://doi.org/10.1021/ja0752835
15. Liu, Y., Willis, M., Rowell, N., Luo, W., Fan, H., Han, S., & Yu, K. (2018). Effect of small molecule additives in the prenucleation stage of semiconductor CdSe quantum dots. *The Journal of Physical Chemistry Letters, 9*(21), 6356–6363. https://doi.org/10.1021/acs.jpclett.8b02371
16. Matea, C. T., Mocan, T., Tabaran, F., Pop, T., Mosteanu, O., Puia, C., Iancu, C., & Mocan, L. (2017). Quantum dots in imaging, drug delivery and sensor applications. *International Journal of Nanomedicine, 12*, 5421–5431. https://doi.org/10.2147/IJN.S138624
17. Milenković, M., Mišović, A., Jovanović, D., Popović Bijelić, A., Ciasca, G., Romanò, S., Bonasera, A., Mojsin, M., Pejić, J., & Stevanović, M. (2021). Facile synthesis of L-cysteine functionalized graphene quantum dots as a bioimaging and photosensitive agent. *Nanomaterials, 11*(8), 1879. https://doi.org/10.3390/nano11081879
18. Mirnajafizadeh, F., Ramsey, D., McAlpine, S., Wang, F., & Stride, J. A. (2019). Nanoparticles for bioapplications: Study of the cytotoxicity of water dispersible CdSe(S) and CdSe(S)/ZnO quantum dots. *Nanomaterials, 9*(3), 465. https://doi.org/10.3390/nano9030465
19. Ngamdee, K., Kulchat, S., Tuntulani, T., & Ngeontae, W. (2017). Fluorescence sensor based on D-penicillamine capped cadmium sulfide quantum dots for the detection of cysteamine. *Journal of Luminescence, 187*, 260–268. https://doi.org/10.1016/j.jlumin.2017.03.051
20. Nikazar, S., Sivasankarapillai, V. S., Rahdar, A., Gasmi, S., Anumol, P., & Shanavas, M. S. (2020). Revisiting the cytotoxicity of quantum dots: An in-depth overview. *Biophysical Reviews, 12*(3), 703–718. https://doi.org/10.1007/s12551-020-00668-6
21. Park, S. W., Kim, T. E., & Jung, Y. K. (2021). Glutathione-decorated fluorescent carbon quantum dots for sensitive and selective detection of levodopa. *Analytica Chimica Acta, 1165*, 338513. https://doi.org/10.1016/j.aca.2021.338513
22. Pu, Y., Cai, F., Wang, D., Wang, J.-X., & Chen, J.-F. (2018). Colloidal synthesis of semiconductor quantum dots toward large-scale production: A review. *Industrial & Engineering Chemistry Research, 57*(6), 1790–1802. https://doi.org/10.1021/acs.iecr.7b04803
23. Sajwan, R. K., Bagbi, Y., Sharma, P., & Solanki, P. R. (2017). L-cysteine and 3-mercaptopropionic acid capped cadmium selenide quantum dots based metal ion probes. *Journal of Luminescence, 187*, 126–132. https://doi.org/10.1016/j.jlumin.2017.03.024
24. Shivaji, K., Balasubramanian, M. G., Devadoss, A., Asokan, V., De Castro, C. S., Davies, M. L., Ponmurugan, P., & Pitchaimuthu, S. (2019). Utilization of waste tea leaves as bio-surfactant in CdS quantum dots synthesis and their cytotoxicity effect in breast cancer cells. *Applied Surface Science, 487*, 159–170. https://doi.org/10.1016/j.apsusc.2019.05.191
25. Tan, X., Liu, S., Shen, Y., He, Y., Liu, Y., & Yang, J. (2014). Glutathione-capped CdTe quantum dots for the determination of fleroxacin with dual-wavelength fluorescence signals. *Analytical Methods, 6*(13), 4860–4866. https://doi.org/10.1039/C4AY00652K
26. Vaishnavi, E., & Renganathan, R. (2020). Quantum dots application in biomolecules interaction and bioimaging. In *Integrative Nanomedicine for New Therapies* (pp. 247–268). Springer. https://doi.org/10.1007/978-3-030-43214-3_10
27. VanWie, T., Wysocki, E., McBride, J. R., & Rosenthal, S. J. (2019). Bright cool white emission from ultrasmall CdSe quantum dots. *Chemistry of Materials, 31*(20), 8558–8562. https://doi.org/10.1021/acs.chemmater.9b02888
28. Vyshnava, S. S., Pandluru, G., Kanderi, D. K., Panjala, S. P., Banapuram, S., Paramasivam, K., Anupalli, R. R., Bontha, R. R., & Dowlatabad, M. R. (2020). Gram scale synthesis of QD 450 core–shell quantum dots for cellular imaging and sorting. *Applied Nanoscience, 10*(4), 1257–1268. https://doi.org/10.1007/s13204-019-01234-z
29. Yu, W. W., Qu, L., Guo, W., & Peng, X. (2003). Experimental determination of the extinction coefficient of CdTe, CdSe, and CdS nanocrystals. *Chemistry of Materials, 15*(14), 2854–2860. https://doi.org/10.1021/cm034081k
30. Zhao, P., Xu, Q., Tao, J., Jin, Z., Pan, Y., Yu, C., & Yu, Z. (2018). Near infrared quantum dots in biomedical applications: Current status and future perspective. *Wiley Interdisciplinary Reviews: Nanomedicine and Nanobiotechnology, 10*(3), e1483. https://doi.org/10.1002/wnan.1483
31. Zheng, Y., Gao, S., & Ying, J. Y. (2007a). Synthesis and cell-imaging applications of glutathione-capped CdTe quantum dots. *Advanced Materials, 19*(3), 376–380. https://doi.org/10.1002/adma.200601447
32. Zheng, Y., Yang, Z., & Ying, J. Y. (2007b). Aqueous synthesis of glutathione-capped ZnSe and Zn1–xCdxSe alloyed quantum dots. *Advanced Materials, 19*(11), 1475–1479. https://doi.org/10.1002/adma.200601878